CHAPTER 3

MANIFOLD FLOW

3.1 INTRODUCTION

Every hydraulic manifold consists of one relatively large pipe, or several in some kind of series configuration, which may be called the barrel or main. Along each main pipe there are numerous junctions with small pipes or there are numerous ports, all allowing flow from the main or (less common) all allowing flow into the main. One characteristic of manifolds is the presence of many junctions or ports, usually relatively closely spaced but not so close that the flow at adjacent ports interacts. Every flow in a manifold is a spatially varied flow, and flows in manifolds are almost always analyzed as steady flows, as we will do in this chapter.

Although manifold flow is a less-frequently studied topic than the flow in networks or the behavior of hydraulic transients, this flow type does have numerous practical applications. Manifold flow has several kinds of applications to farm irrigation systems (Jensen, M. E., 1983; U. S. Soil Conservation Service, 1984; James, L. G., 1988; Cuenca, R. H., 1989; Keller, J. and Bliesner, R. D., 1990), including recent research on trickle and sprinkler systems (e.g., Scaloppi, E. J. and Allen, R. G., 1993; Hathoot, H. M. et al., 1994). Protective fire sprinkler systems in buildings are another application. Marine outfall systems (Vigander, S. et al., 1970; Grace, R. A., 1978) rely on manifolds for the initial distribution of the wastewater into the receiving water body through multi-port diffuser manifolds. The filling and emptying systems for large locks on navigable waterways are basically manifolds (Richardson, G. C., 1964, 1969; Stockstill, R. L. et al., 1991). And the ventilation of vehicle tunnels also relies in part on an understanding of manifold flow (Pursall, B. R. and King, A. L., 1976).

This chapter will first describe several levels of analysis that are applicable to manifold flow; they differ in whether friction is considered and whether junction losses are considered. We will then look at one example of an analysis of the internal hydraulics of a marine outfall diffuser and show how this approach can easily be aided with a short computer program. Articles by McNown (1954) and Rawn et al. (1961) and the book by Miller (1984) are good places to begin further study of this topic.

3.2 ANALYSIS OF MANIFOLD FLOW

In this section we will look at the analysis of flow in a manifold on three levels. The first level will ignore all energy losses; although this assumption is unrealistic, it will serve as an introduction to manifold flow and allow us to unlearn some flow behavior from the flow in pipes which is not spatially varied. In the second and third levels we progressively add friction in the barrel or main, and a consideration of energy losses at junctions or ports. At the end of these analyses we can draw some conclusions about the importance of barrel friction and junction losses in various applications.

3.2.1. NO FRICTION

Primarily as an introduction to the subject, let us look briefly at the schematic diagram of a small, simple manifold having only a few equally-spaced circular exit ports, all of the same diameter, as shown in Fig. 3.1. The downstream end of the main is a dead end. In the complete absence of real-fluid effects, the reservoir level on the left sets the elevation of

the horizontal energy line along the entire manifold, which is shown here as having five single exit ports that are relatively closely spaced. A sectional view is shown on the right,

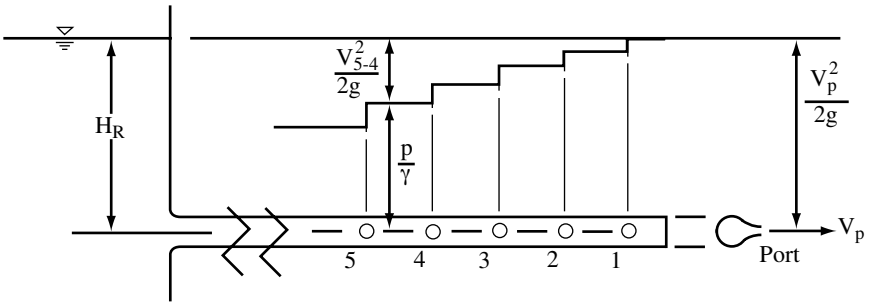

Figure 3.1 A small manifold, no pipe friction or junction losses.

with the transition region from the main to the exit point being rounded to suggest that energy losses in the port region can indeed be neglected as a first approximation. For convenience in the analyses, the ports are numbered from the downstream end toward the reservoir, beginning with 1. The key feature here is the behavior of the hydraulic grade line for this flow. As always, we can locate the hydraulic grade line by measuring down a distance of $V^2/2g$ from the energy line to it, in which V is the mean velocity in the barrel segment. Since this mean velocity becomes progressively larger as we move from the lower- to higher-numbered ports, the hydraulic grade line, and therefore the pressure head p/γ, is farthest below the energy line at the upstream end of the barrel. Since it is usual to think of the pressure in a horizontal pipe as decreasing in the direction of flow, we have an immediate indication that some care will be required if we are to avoid reaching incorrect conclusions as we study manifold flow.

In the absence of energy losses, the velocity from each port is $V_p = [2gH_R]^{1/2}$. The discharge from each port is then identical if the ports are all the same. With identical ports, only two factors can cause the discharge to change from port to port: differing energy levels from port to port, and junction energy losses. We shall look at both factors in the next two sections.

A reading of past literature will reveal two points of view on the physics of the flow out of a port: Some articles assume that only the pressure head in the main is responsible for driving the fluid out of an adjacent port. Others, including this text, write a work-energy equation between the main and the exit point of the port; this approach assumes that the full distance between the EL in the main and the exit point drives the flow. The existence of loss coefficients and discharge coefficients, which play somewhat differing roles, depending on the point of view, allows the two approaches to be made compatible with one another.

3.2.2. BARREL FRICTION ONLY

When barrel friction is considered, then the energy line slopes downward as a sequence of straight-line segments in the direction of flow in the barrel, as shown in Fig. 3.2. As we look from port 1 to port 5, we find the velocity head in the barrel grows as it did in the absence of friction, and each segment of the hydraulic grade line along the barrel also has a slope that is parallel to the energy line above it. We find the port velocity is $V_{pi} = [2gH_i]^{1/2}$, in which H_i is the vertical distance from the centerline of port i to the local energy line above that port. And the discharge in the barrel changes in each segment, in accordance with continuity at each junction.

In the manifold section of length L with five equally-spaced ports, we may record the frictional head loss as

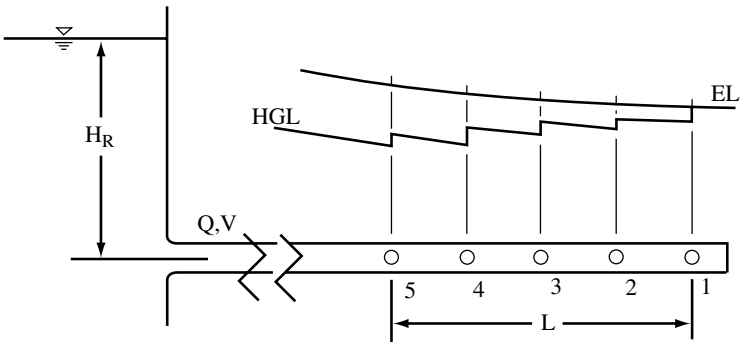

Figure 3.2 A small manifold, $n = 5$ ports, with barrel friction but no junction losses.

$$\sum h_L = f\frac{L/4}{D}\frac{V_{5-4}^2}{2g} + f\frac{L/4}{D}\frac{V_{4-3}^2}{2g} + f\frac{L/4}{D}\frac{V_{3-2}^2}{2g} + f\frac{L/4}{D}\frac{V_{2-1}^2}{2g} \tag{3.1}$$

if we assume that the pipe Reynolds number is sufficiently high that the Darcy-Weisbach friction factor f is a constant over the range of flow in the barrel.

Various results can be developed from Eq. 3.1 or an equation like it, depending on the diameters of the ports. For example, with a total discharge Q_T and the assumption that the diameter of each port is chosen so that equal discharges issue from each of the five ports, that is, $Q_p = Q_T/5$, then in each barrel segment port continuity shows that $V_{5\text{-}4} = 4V/5$, $V_{4\text{-}3} = 3V/5$, $V_{3\text{-}2} = 2V/5$, and $V_{2\text{-}1} = V/5$. Then Eq. 3.1 will simplify to

$$\sum h_L = \frac{1}{4}\left[\left(\frac{4}{5}\right)^2 + \left(\frac{3}{5}\right)^2 + \left(\frac{2}{5}\right)^2 + \left(\frac{1}{5}\right)^2\right] f\frac{L}{D}\frac{V^2}{2g} = 0.3f\frac{L}{D}\frac{V^2}{2g} \tag{3.2}$$

with $V = Q_T/A$ and A = cross-sectional area of the main. If instead there were n ports with equal discharges $Q_p = Q_T/n$, then by using mathematical induction we find that the total frictional head loss for the section of the main containing the ports is

$$\sum h_L = \frac{1}{n-1}\left[\frac{1}{n^2}\sum_{i=1}^{(n-1)} i^2\right] f\frac{L}{D}\frac{V^2}{2g} = \frac{1}{n-1}\left[\frac{1}{n^2}\frac{n}{6}(n-1)(2n-1)\right] f\frac{L}{D}\frac{V^2}{2g} \tag{3.3}$$

or

$$\sum h_L = \left(\frac{1}{3} - \frac{1}{6n}\right) f\frac{L}{D}\frac{V^2}{2g} \tag{3.4}$$

However, the unhappy fact is that the diameter of each port must differ, if only slightly, from the diameters of the other port openings for this expression to be completely applicable. But Eq. 3.4 may still be useful in obtaining an approximation for the head loss over a group of n uniformly spaced ports in a distance L in a barrel.

3.2.3. BARREL FRICTION WITH JUNCTION LOSSES

Now the state of affairs at the intersection of the barrel and a pipe lateral of smaller diameter, both assumed here to lie in one horizontal plane, is relatively complex. We begin with a diagram, Fig. 3.3, of one such barrel-lateral junction that displays the energy line EL and hydraulic grade line HGL for the main and the lateral and also introduces a set of locally-numbered variables: subscript 1 denotes a variable that is defined upstream of the lateral in the main; subscript 2 denotes a variable that is defined downstream of the

lateral in the main; and subscript 3 denotes a variable that is associated with the lateral itself. It is assumed that the spacing of the laterals is such that the flow to successive laterals does not interact. The energy line now has a loss $h_{L_{1-2}}$ along the main at the junction, and there is also an energy loss $h_{L_{1-3}}$ at the junction that is associated with the flow that passes into the lateral. The hydraulic grade line experiences a rise Δh along the main as it passes the junction. We must keep in mind that it is the art/science of approximation in hydraulics that expresses these energy and pressure changes as discrete jumps at a precise location; actually all three factors represent phenomena that occur over a larger but finite flow region, although we concentrate or lump the effect at a point. All parts of the energy line slope downward in the direction of flow in the main and in the lateral, owing to the

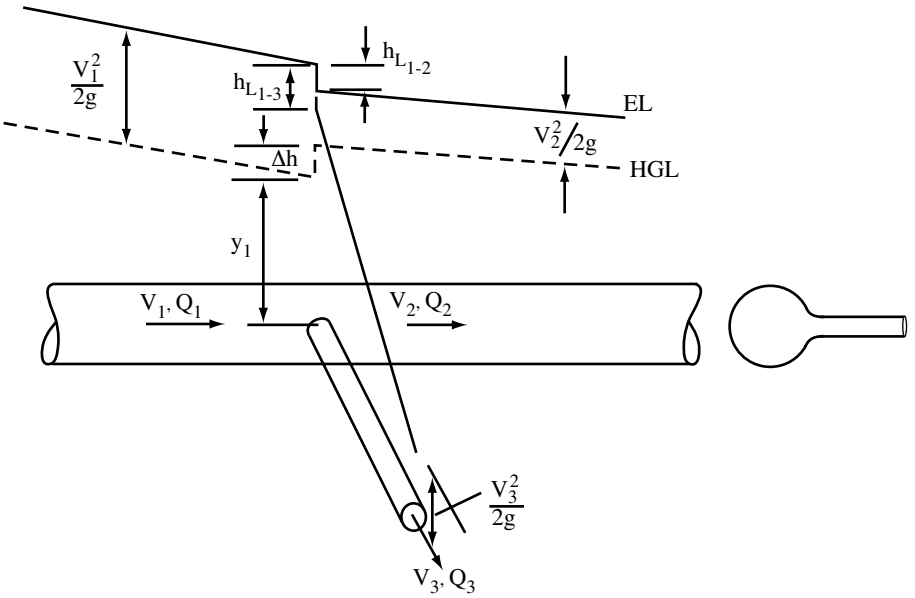

Figure 3.3 Diagram of a barrel-lateral junction with local notation.

effect of fluid friction. The flow from the lateral is presumed to exit as a jet into the atmosphere.

From Fig. 3.3 we see that the pressure head rise along the main is

$$\Delta h = \frac{V_1^2}{2g} - \frac{V_2^2}{2g} - h_{L_{1-2}} \tag{3.5}$$

Dividing all by the upstream velocity head produces a nondimensional pressure head rise coefficient

$$\frac{\Delta h}{V_1^2/2g} = 1 - \left(\frac{V_2}{V_1}\right)^2 - \frac{h_{L_{1-2}}}{V_1^2/2g} \tag{3.6}$$

or

$$\frac{\Delta h}{V_1^2/2g} = 1 - \left(\frac{Q_2}{Q_1}\right)^2 - \frac{h_{L_{1-2}}}{V_1^2/2g} \tag{3.7}$$

Applying continuity at the junction in the form $Q_1 = Q_2 + Q_3$ leads to

$$\frac{\Delta h}{V_1^2/2g} = 1 - \left(1 - \frac{Q_3}{Q_1}\right)^2 - \frac{h_{L_{1-2}}}{V_1^2/2g} = 2\left(\frac{Q_3}{Q_1}\right) - \left(\frac{Q_3}{Q_1}\right)^2 - \frac{h_{L_{1-2}}}{V_1^2/2g} \tag{3.8}$$

If we employ the usual terminology, the last term in Eq. 3.8 is the head loss coefficient $K_{L_{1-2}}$. Hence we can conclude that the pressure head rise coefficient is a function of only two nondimensional factors, or

$$\frac{\Delta h}{V_1^2/2g} = \Phi_1\left(\frac{Q_3}{Q_1}, \frac{h_{L_{1-2}}}{V_1^2/2g}\right) \tag{3.9}$$

in which Φ_1 is the function appearing in Eq. 3.8.

Statements about the functional behavior of the pressure head rise coefficient can be made if we hypothesize how $h_{L_{1-2}}$ behaves; Figure 3.4 is the outcome of such an inquiry.

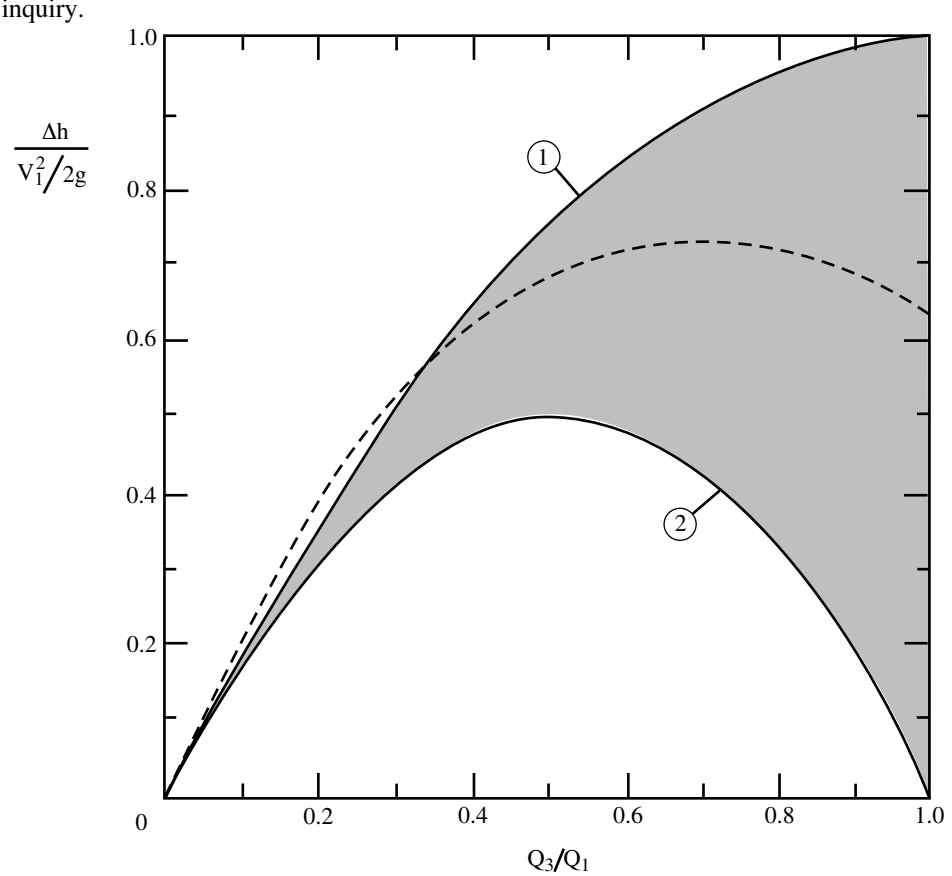

Figure 3.4 The expected range of pressure rise coefficients as a function of Q_3/Q_1.

To begin probing this point, it does not seem difficult to delimit the range of possible values for $h_{L_{1-2}}$. At the low end it seems reasonable simply to assume $(h_{L_{1-2}})_{min} = 0$, i.e., no loss. At the high end of the spectrum we note that the flow in the main at the

junction displays some of the character of the flow at a sudden enlargement, as a rapid deceleration of the flow occurs in the barrel, accompanied by some increase in eddy motion and other turbulence phenomena. Hence we expect

$$\left(h_{L_{1-2}}\right)_{max} = \frac{\left(V_1 - V_2\right)^2}{2g} \tag{3.10}$$

This behavior for the pressure head rise coefficient is plotted in Fig. 3.4 as a function of the discharge ratio Q_3/Q_1; curve 1 is the curve for minimum head loss, and curve 2 is the result of using Eq. 3.10 to represent the head loss. Superimposed on Fig. 3.4 is a dashed curve that is taken from Fig. 3.5, which shows experimental data (unpublished) for the typical behavior of the pressure head rise coefficient as a function of the lateral-to-main diameter ratio D_3/D_1, assuming in this example that $f = 0.02$ and $L_3/D_3 = 5$ for the lateral.

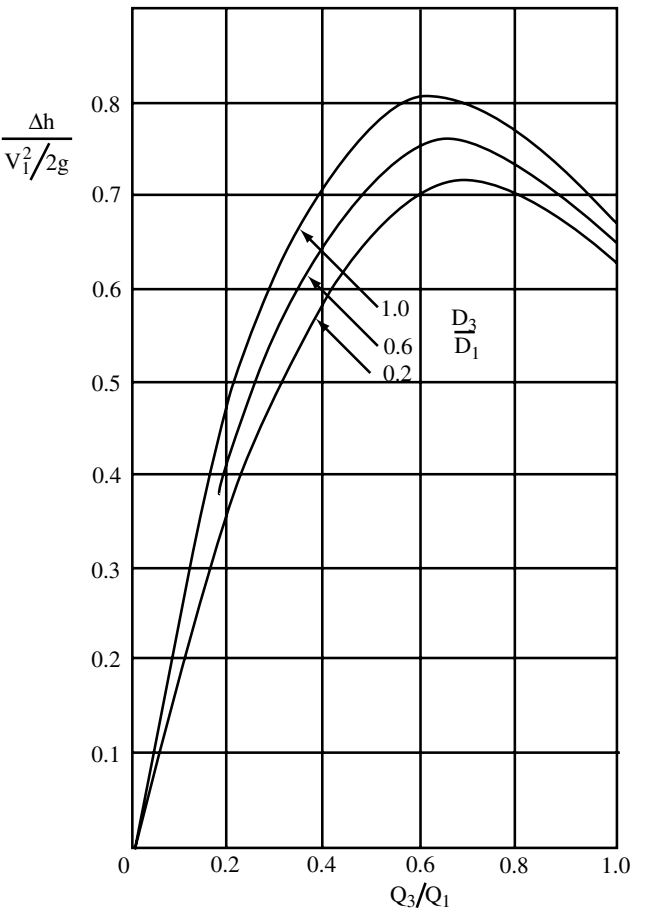

Figure 3.5 Typical experimental data for the pressure rise coefficient.

From Fig. 3.4 we find a remarkable result. The experimental pressure head rise coefficient data do not fall within the rather generous region of expected behavior for D_3/D_1 below about 1/3. The clear meaning is that the loss coefficient $K_{L_{1-2}}$ is negative for small values of D_3/D_1. How can this be? It is not simply caused by

experimental error but is a real phenomenon, another of the peculiarities of manifold flow, the cause of which has been debated at some length. Experts conclude that the flow must be something like the diagram in Fig. 3.6, in which a small fraction of the upstream discharge is drawn into the lateral. This lateral fraction initially possessed less than the average kinetic energy per unit weight of fluid, since the fluid near the pipe wall moves more slowly than the central core fluid. Consequently the mean energy that remains to flow to section 2 appears to have been enhanced by a small amount. In a one-dimensional hydraulic representation of the flow, the effect shows up as a small "negative" loss coefficient, however unrealistic that may seem. Additional study would show that a loss in the overall flux of energy does still occur in this situation.

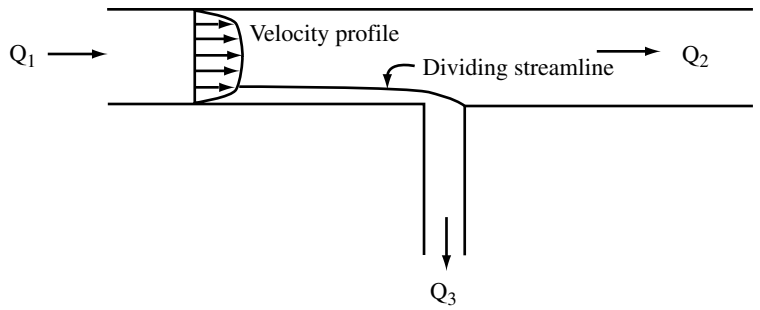

Figure 3.6 Flow at a lateral junction.

The behavior of the flow in the lateral must also be quantified. The habit began long ago of treating these laterals as if they were orifices and assuming for convenience that the flow through the lateral was driven by the pressure head y_1 that exists just upstream from the entrance to the lateral. Thus we write

$$Q_3 = CA_3\sqrt{2gy_1} \quad \text{or} \quad y_1 = \frac{1}{C^2}\frac{V_3^2}{2g} \tag{3.11}$$

in which $A_3 = \pi D_3^2/4$ is the cross-sectional area of a lateral of diameter D_3, the velocity $V_3 = Q_3/A_3$, and C is the orifice coefficient, which can depend on several variables, depending on the geometric details of the lateral.

We want to establish a relation between C and the head loss coefficient $K_{L_{1-3}}$ for flow from the main to the lateral

$$K_{L_{1-3}} = \frac{h_{L_{1-3}}}{V_1^2/2g} \tag{3.12}$$

since this coefficient can be found experimentally. Assuming that the lateral flows full and has length L_3 and a constant friction factor f_3, from Fig. 3.3 we can write

$$y_1 + \frac{V_1^2}{2g} = h_{L_{1-3}} + h_{f_3} + \frac{V_3^2}{2g} \tag{3.13}$$

with h_{f_3} being the frictional head loss in the lateral, or

$$\frac{1}{C^2}\frac{V_3^2}{2g} + \frac{V_1^2}{2g} = K_{L_{1-3}}\frac{V_1^2}{2g} + f_3\frac{L_3}{D_3}\frac{V_3^2}{2g} + \frac{V_3^2}{2g} \tag{3.14}$$

Dividing throughout by the velocity head in the lateral and rearranging,

$$\frac{1}{C^2} = \left(K_{L_{1-3}} - 1\right)\left(\frac{V_1}{V_3}\right)^2 + \left(1 + f_3 \frac{L_3}{D_3}\right) \tag{3.15}$$

or

$$\frac{1}{C^2} = \left(K_{L_{1-3}} - 1\right)\left(\frac{Q_1}{Q_3}\right)^2 \left(\frac{D_3}{D_1}\right)^4 + \left(1 + f_3 \frac{L_3}{D_3}\right) \tag{3.16}$$

In summary,

$$C = \Phi_2\left(\frac{Q_3}{Q_1},\ K_{L_{1-3}}\right) \tag{3.17}$$

in which Φ_2 is a shorthand notation for the function displayed in full in Eq. 3.16. When

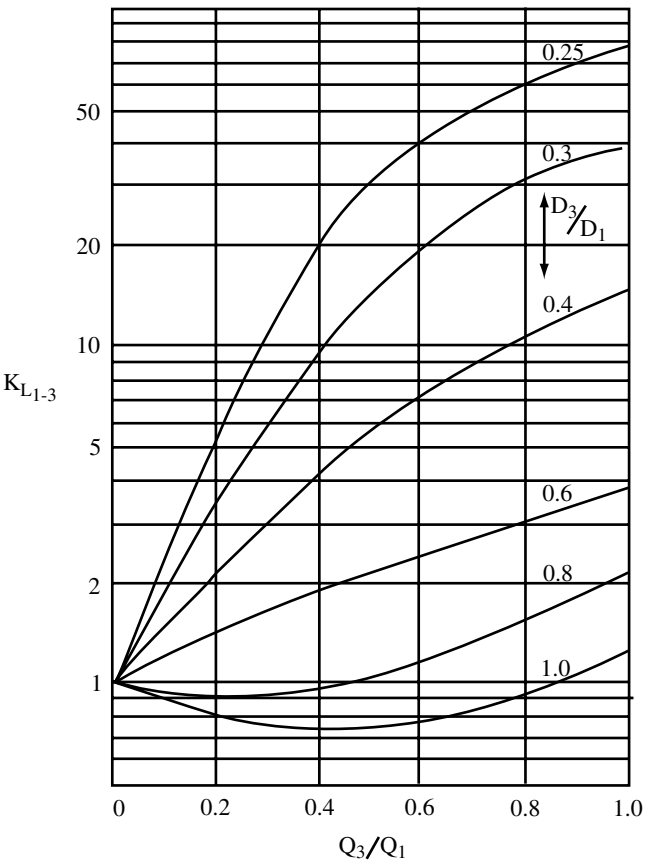

Figure 3.7 The loss coefficient $K_{L_{1-3}}$ as a function of D_3/D_1 and Q_3/Q_1.

appropriate experiments have been conducted to determine the behavior of $K_{L_{1-3}}$, one will usually find a relation that is similar to that shown in Fig. 3.7. And once f_3 and L_3/D_3 have been prescribed, then a plot of C vs. Q_3/Q_1 can be prepared; for example, Fig. 3.8 has been prepared from Fig. 3.7 by assuming $f_3 = 0.02$ and $L_3/D_3 = 5$. (Some will be surprised to see how large the lateral loss coefficient may become; keep in mind, however, that a lateral that is less than 1/3 the diameter of the main will normally convey

1/3 or less of the upstream discharge to that junction, so such high loss coefficients are rarely encountered in practice.)

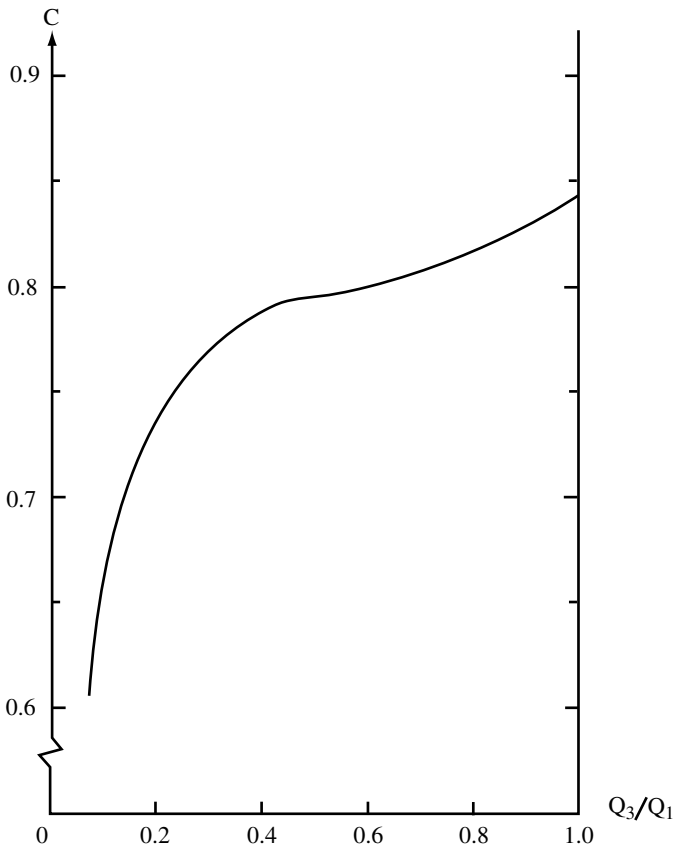

Figure 3.8 An example of the behavior of the orifice coefficient C.

Example Problem 3.1

The 3-port manifold shown in the next diagram has a port-to-main diameter ratio $D_3/D_1 = D_3/D_m = 0.4$, a friction factor $f = 0.02$ in the main and all laterals, and $L_3/D_3 = 5$ for each lateral. Considering fluid friction in the main and laterals and junction losses, as described by Figs. 3.5, 3.7, and 3.8, compute the port discharges Q_a, Q_b, and Q_c. The downstream end of the main is closed off by a blank plate.

This problem is more difficult than earlier problems where the junction losses were ignored, but the results are valuable in helping us decide whether to include or ignore junction losses in other similar problems.

Such a problem can be formulated in terms of a set of linear and nonlinear simultaneous equations, but in the past solutions to this problem were normally sought by following the

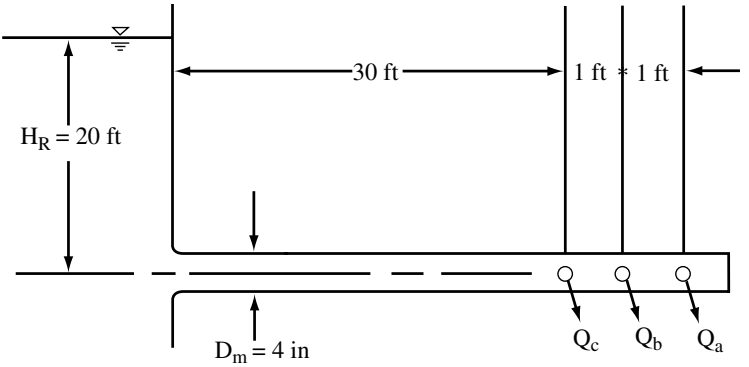

method that will now be used. The solution process typically begins by arbitrarily selecting an energy line elevation at the downstream end of the manifold, and computations are started there. Of course, the initial elevation will almost never be the correct final elevation, but it is easy to adjust for this later in the computations. So we begin by choosing EL = HGL = 10.0 ft downstream of port 1.

At port a the ratio $Q_{lateral}/Q_{main} = Q_3/Q_1 = Q_a/Q = 1.0$. Just before this port we see that $y_1 + \Delta h = 10.00$, with the discharge out the first port satisfying

$$Q_a = Q_3 = C\frac{\pi D_3^2}{4}\sqrt{2gy_1}$$

From Fig. 3.5 we read $\dfrac{\Delta h}{V_1^2/2g} = 0.63$, and from Fig. 3.8 we find $C = 0.84$. Hence

$$\left(\frac{Q_a}{0.84}\frac{4}{\pi D_3^2}\right)^2\frac{1}{2g} + 0.63\left(\frac{4Q_a}{\pi D_m^2}\right)^2\frac{1}{2g} = 10.00$$

with $D_3 = 0.4(4)/12 = 0.1333$ ft and $g = 32.2$ ft/s^2. From this equation we compute $Q_a = 0.296$ ft^3/s, from which $V_1^2/2g = 0.179$ ft and $\Delta h = 0.113$ ft, which establishes the values of the EL and HGL immediately before port a as 10.066 ft and 9.887 ft, respectively. With these values the frictional loss between port a and port b is 0.011 ft from the Darcy-Weisbach equation, giving EL and HGL elevations of 10.077 ft and 9.898 ft just downstream of port b.

With no prior experience upon which to anticipate the flow behavior at port b, the second port, the logical initial estimate for the discharge ratio is $Q_{lateral}/Q_{main} = Q_b/Q = 0.50$. Turning to the plots, from Fig. 3.5 we obtain $\dfrac{\Delta h}{V_1^2/2g} = 0.680$ and from Fig. 3.8 $C = 0.795$. With $Q = Q_b/0.5$, the equation $y_1 + \Delta h = 9.898$ ft at port b becomes

$$\left(\frac{Q_b}{0.795}\frac{4}{\pi D_3^2}\right)^2\frac{1}{2g} + 0.680\left(\frac{4(Q_b/0.5)}{\pi D_m^2}\right)^2\frac{1}{2g} = 9.898$$

or $Q_b = 0.274$ ft^3/s. The discharge in the main is then $0.296 + 0.274 = 0.570$ ft^3/s and $Q_b/Q = 0.274/0.570 = 0.481$, which is not 0.50 as assumed. Thus we repeat the calculation using $Q_b/Q = 0.481$, with 0.670 being read with some difficulty from Fig.

3.5 and $C = 0.795$ from Fig. 3.8. Also the discharge in the main shifts slightly to become $Q = Q_b/0.481 = 2.08Q_b$. The new result is $Q_b = 0.274$ ft^3/s again. For this discharge we can compute $V_1^2/2g =$ 0.662 ft and $\Delta h =$ 0.444 ft with $y_1 = 9.465$ ft, leading to EL and HGL elevations just before port b of 10.127 ft and 9.465 ft. The Darcy-Weisbach frictional loss between port b and port c is then 0.040 ft so that the EL and HGL elevations just downstream of port c are 10.167 ft and 9.505 ft.

At port c the uninformed initial estimate for the discharge ratio would be $Q_c/Q = 0.333$. But from our experience at port b we may speculate that this ratio will be too high and instead choose our first estimate to be $Q_c/Q = 0.31$ so that $Q = Q_c/0.31 = 3.23Q_c$. Then Fig. 3.5 yields $\dfrac{\Delta h}{V_1^2/2g} = 0.545$, and $C = 0.770$ is obtained from Fig. 3.8. The equation $y_1 + \Delta h = 9.505$ ft at port c is then

$$\left(\frac{Q_c}{0.770}\,\frac{4}{\pi D_3^2}\right)^2 \frac{1}{2g} + 0.545\left(\frac{4(3.23Q_c)}{\pi D_m^2}\right)^2 \frac{1}{2g} = 9.505$$

giving $Q_c = 0.255$ ft^3/s. Then in the main $Q = 0.570 + 0.255 = 0.825$ ft^3/s, with a ratio $Q_c/Q = 0.255/0.825 = 0.31$. We have been fortunate in our choice of the estimate! Otherwise we must repeat the computational cycle of adjusting the discharge ratio and the coefficients that depend on it before again computing a new discharge at port c and checking the result for adequacy. By now it should be clear that a limiting factor in our ability to obtain an accurate solution that agrees with our starting estimates is the accuracy of the coefficients. Two factors affect this accuracy, the quality of the original experiments that led to the preparation of the coefficient plots and our limited ability to read those plots. As a result, Miller (1984) suggested that agreement within 2% is a reasonable goal. At least some of the computations in this example exceed this limit, but the results have been presented in this way so the computations can be followed more easily.

Some computations upstream of port c remain. With the discharge upstream of port c now computed, the velocity head in the main in this region is $V^2/2g = 1.388$ ft, and y_1 upstream of port c is

$$y_1 = \frac{1}{2g}\left(\frac{0.255}{(0.770)(0.01396)}\right)^2 = 8.739 \text{ ft}$$

The EL at this section is the sum of these two terms, or 10.127 ft. Just downstream of port c the EL was computed as 10.167 ft., so we observe the phenomenon of an apparent negative head loss occurring at port c. This effect is small, but it is not an error. Continuing, we compute the effect of the frictional head loss in 30 ft of pipe leading to the reservoir as

$$h_L = f\frac{L}{D}\frac{V^2}{2g} = 0.02\left(\frac{30}{4/12}\right)(1.388) = 2.498 \text{ ft}$$

so that the computed EL at the reservoir is 10.127 + 2.498 = 12.625 ft. Alas, this value is actually specified as $H_R = 20$ ft. Our work is not wasted, however. Each velocity, and consequently each discharge, is proportional to the square root of the total head that is available in the problem, so long as f is assumed to be a constant. To adjust our estimated discharges to the true discharges, we need only multiply the estimates by the

square root of the ratio of the true total head, 20 ft, to the computed head, 12.625 ft. The discharge from each port, in ft^3/s, is therefore

$$Q_{true} = Q_{est}\left[\frac{H_{true}}{H_{est}}\right]^{1/2}$$

$$Q_a = 0.296\left[\frac{20.0}{12.625}\right]^{1/2} = 0.373 \text{ ft}^3/\text{s}$$

$$Q_b = 0.274\left[\frac{20.0}{12.625}\right]^{1/2} = 0.345 \text{ ft}^3/\text{s}$$

$$Q_c = 0.255\left[\frac{20.0}{12.625}\right]^{1/2} = 0.321 \text{ ft}^3/\text{s}$$

If it is desired, the actual elevation of each point on the EL and HGL could now be computed directly since the discharges are known.

The foregoing hand solution has acquainted us with the complexities that come with the inclusion of junction losses. The modern alternative to such a solution is to formulate the problem in terms of a set of equations that can be solved simultaneously for a chosen set of unknown variables. The CD contains both a MathCAD and a TK-Solver model of this problem, listed under the names PRB3_1.MCD and PRB3_1.TK, respectively, which are formulated in this way. For this example we denote the hydraulic grade line downstream ($y_1 + \Delta h$) from the three ports by HGL$_a$, HGL$_b$ and HGL$_c$. In a similar way the C's from Fig. 3.8 and the coefficients K from Fig. 3.5 will be given subscripts a, b, and c. The following three equations are the result of adding y_1 and Δh at the three ports:

$$\left(Q_a/C_a\right)^2/\left(2gA_a^2\right) + K_aQ_a^2/\left(2gA_m^2\right) = HGL_a$$

$$\left(Q_b/C_b\right)^2/\left(2gA_a^2\right) + K_b\left(Q_a + Q_b\right)^2/\left(2gA_m^2\right) = HGL_b$$

$$\left(Q_c/C_c\right)^2/\left(2gA_a^2\right) + K_c\left(Q_a + Q_b + Q_c\right)^2/\left(2gA_m^2\right) = HGL_c$$

in which $A_a = (\pi/4)D_3^2$ is the area of each equally-sized port, and $A_m = (\pi/4)D_m^2$. Along the main three energy equations

$$HGL_b = HGL_a + \left(fL_s/D_m - K_a\right)Q_a^2/\left(2gA_m^2\right)$$

$$HGL_c = HGL_b + \left(fL_s/D_m - K_b\right)\left(Q_a + Q_b\right)^2/\left(2gA_m^2\right)$$

$$H_R = HGL_c + \left(1 + fL/D_m - K_c\right)\left(Q_a + Q_b + Q_c\right)^2/\left(2gA_m^2\right)$$

can be written, in which $L_s = 1$ ft is the spacing between ports, $L = 30$ ft is the length of the upstream main, and $H_R = 20$ ft is the elevation of the reservoir water surface. These six equations can be solved for six variables, which could be chosen as Q_a, Q_b, Q_c, HGL$_a$, HGL$_b$, and HGL$_c$. Using any software that is capable of solving a nonlinear system of equations produces $Q_a = 0.373$ ft^3/s, $Q_b = 0.345$ ft^3/s, $Q_c = 0.321$ ft^3/s, HGL$_a$ = 15.844 ft, HGL$_b$ = 15.683 ft, and HGL$_c$ = 15.043 ft, if the coefficients that were determined in the hand solution are used. If the source of these coefficients must be Figs. 3.5 and 3.8, a solution can be obtained with trial coefficient values, the coefficients can then be adjusted and improved, and the problem can be solved again. However, an

improved computational approach would use "list functions" that would obtain the coefficients from values that are found from tables that describe the curves in these figures. If a function subprogram that solves the Colebrook-White equation (so one Colebrook-White equation would be written to determine the friction factor f in each flow segment of the main; in this case three equations) is added to the equation system, then one could merely specify the pipe material (actually the equivalent sand grain roughness e for that material) rather than specifying a value for f itself. Talozi (1998) has analyzed manifold flow recently using some of these computational approaches.

* * *

A review of these computations allows us to come to several conclusions:

1. As the local ratio Q_3/Q_1 changes, the experimentally determined coefficients that describe the flow at each junction probably also change. The flow from a port cannot be determined accurately unless the lateral discharge coefficient C and the nondimensional pressure head rise coefficient are known reasonably well.
2. For practical manifold flows in which a large number (more than three or four is large) of ports are present, the negative head loss phenomenon will in theory be present at a large majority of the ports (all but the last few ports), but the actual amount of the energy change across such a port will almost always be very small. And if this energy change (gain) across a port along the main is neglected, the effect of this neglect is a conservative one in the design process.
3. The first end-of-chapter problems will demonstrate that ports of equal diameter, in the absence of the consideration of junction losses, display a trend of increasing port discharge with increasing EL in the main. But Example Problem 3.1 is one example where a consideration of junction losses leads to a decrease in port discharge with an increasing EL as one moves upstream. When this trend was observed many years ago along with a decrease in pressure head in the upstream direction, it was concluded that it was the pressure head, and not the energy line location, that determined the port discharge; old technical articles that emphasize the importance of pressure head alone in manifold behavior should be viewed with caution.

3.3 A HYDRAULIC DESIGN PROCEDURE

Whether the application is a submarine diffuser as part of a wastewater dispersal operation or a drip irrigation system, some elements of the design procedure change little. There are also some elements that vary from application to application, however. A submarine diffuser, for example, normally is laid on a slope in water of a different density than that of the wastewater, which leads to external pressure differences from port to port that must be incorporated into the design computations. And the physical shape of a submarine diffuser port differs substantially in size and other details from, say, a drip irrigation emitter (port). With some exceptions the trend in recent years is toward a larger number of smaller ports. And the ports within a major segment of the manifold, if not the entire manifold, will be uniformly spaced and of uniform diameter for ease of construction.

In the design of a manifold there are several goals:

1. To assure that the manifold functions in the intended manner, it must always flow full. For a simple manifold this is usually met by requiring the sum of the individual port cross-sectional areas to be less than, typically about 90% of, the cross-sectional area of the main. For larger manifolds with a stepped main, the ratio of the sum of port areas downstream from a particular section to the cross-sectional area of the main at that section is usually limited to some fraction between 1/2 and 2/3.

2. The ports and the main should both have a simple, clean design for several reasons. A simple design will often lead to low hydraulic losses, which will reduce operating expense by saving energy and will lead to a much simpler hydraulic analysis if junction losses can be neglected. It ought also to reduce maintenance costs.
3. The primary design goal, but not one that is strictly attainable, is an even or relatively even distribution of flow between ports.
4. The range of acceptable velocities in the main should be examined carefully for each application, especially if there is any possibility of some solids being conveyed in the manifold. The velocity of the carrier fluid must then be high enough to prevent the settlement of the solids, and it must also be low enough to avoid a scour or abrasion problem. When solids are borne in water, the acceptable range is between 2 and 15 ft/s but usually below 5 ft/s.

The computational sequence for manifold design that will be described in the following paragraphs was developed in the 1960s and 1970s by several investigators and authors, including Rawn et al. (1960), Vigander et al. (1970), and Grace (1978). A brief look into these publications, however, will show the continuing influence of N. H. Brooks on all these efforts. Notationally we follow the presentation of Grace (1978), which is diagramed in Fig. 3.9. The procedure is organized so the entire sequence can be converted relatively directly into computer code.

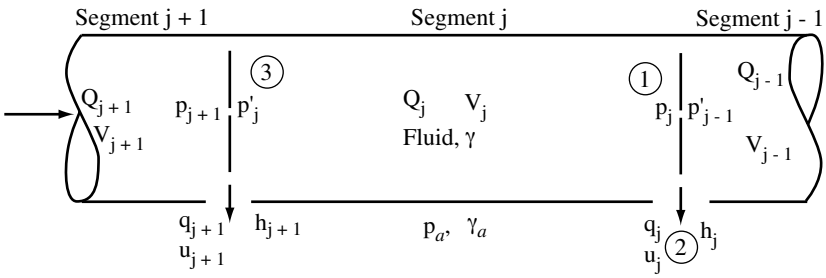

Figure 3.9 A two-port segment of a manifold, to display notation.

The manifold ports and barrel segments are numbered from the downstream end toward the upstream supply head or reservoir, with each port and segment number that is upstream of it denoted by j, which will also be used as a subscript on the other variables to indicate their location. Other variables are Q = discharge in the barrel segment, V = mean velocity in the barrel segment, A = cross-sectional area of the barrel segment, D = diameter of the barrel segment, q = discharge from a port, u = mean velocity through a port, a = cross-sectional area of a port, and d = diameter of a port.

To allow several different design environments, we assume that this design considers a manifold or diffuser conveying a liquid fluid of constant unit weight γ (the fluid is usually water, but the design procedure is not restricted to water only) that is submerged in an ambient body of fluid of constant unit weight γ_a. The horizontal surface of the exterior fluid body serves as a datum where $h = 0$; the submerged elevation of a port is then $-h$, which will change from port to port if the manifold slopes. The pressure outside a port is $p_a = \gamma_a h$. If the ambient fluid is air, then we choose $\gamma_a = 0$. The hydraulic model of flow in a manifold has a discrete jump in pressure across a port; just upstream of port j the internal pressure is p_j, and just downstream of the next port the pressure is p'_j. Flow is assumed to exit horizontally from ports having centerlines at the same elevation as the centerline of the barrel.

The manifold computations begin at the downstream end. Select an estimate of the average port discharge q_p as the total discharge through the manifold divided by the

number of ports. If the fluid flow in the manifold is to carry with it any settleable material, then it is advisable to put a large port, with a discharge of roughly $4q_p$, at the downstream end to counteract the siltation that would otherwise occur in a dead end. The discharge through this port is governed by an orifice equation, but the total head at this port is not known; simply pick a value for the total head that is consistent with the port discharge that is chosen, and it will be corrected later.

The computations at a port, say port j, are basically the same for every port. We write an energy equation from a point inside the main, point 1, to a point in the port efflux stream, point 2:

$$-h_j + \frac{V_j^2}{2g} + \frac{p_j}{\gamma} = -h_j + \frac{u_j^2}{2g} + \frac{p_{aj}}{\gamma} + k_L \frac{u_j^2}{2g} \tag{3.18}$$

In this equation k_L is the port head loss coefficient. If we define an energy parameter E at port j as

$$E_j = \frac{p_j - p_{aj}}{\gamma} + \frac{V_j^2}{2g} \tag{3.19}$$

then the fluid exit velocity through the port is

$$u_j = \left(\frac{1}{1+k_L}\right)^{1/2} \left(2gE_j\right)^{1/2} \tag{3.20}$$

The discharge through this port is the product of the port velocity and the flow cross-sectional area of the jet from this port, or

$$q_j = u_j C_c a_j \tag{3.21}$$

or

$$q_j = C_D a_j \left(2gE_j\right)^{1/2} \tag{3.22}$$

with the discharge coefficient C_D combining the effects of the port head loss and the local contraction coefficient C_c into

$$C_D = C_c / \left(1+k_L\right)^{1/2} \tag{3.23}$$

Since the local loss coefficient varies, for an unchanging individual port geometry, with the ratio of the local velocity head to total head or its surrogate E_j, these relations can be contracted to

$$C_{Dj} = C_D \left(\frac{V_j^2/2g}{E_j}\right) \tag{3.24}$$

This function must initially be determined experimentally, and the results can be summarized in any number of ways, in a graph or table, as an analytical curve fit or as data pairs that can be interpolated by a computer program subroutine. For example, Grace (1978) cites an empirical equation fitting data that describe the flow through a bell-mouth port that is part of the diffuser manifold in an ocean outfall for the city of Honolulu, valid only when $d_j/D_j < 0.1$, as

$$C_D = 0.975\left(1 - \frac{V_j^2/2g}{E_j}\right)^{3/8} \tag{3.25}$$

and Rawn et al. (1960, p. 94) graphically present analogous curves for bell-mouth and sharp-edged ports.

Along the main between points 3 and 1, we may write the energy equation as

$$-h_{j+1} + \frac{V_j^2}{2g} + \frac{p_j'}{\gamma} = -h_j + \frac{V_j^2}{2g} + \frac{p_j}{\gamma} + h_{Lj} \tag{3.26}$$

The velocity head terms cancel, the elevation terms are either known or zero, the pressure head term at port j has been computed, and the last term, the frictional loss term along the barrel, can be computed from the Darcy-Weisbach equation. Hence the pressure head term p_j'/γ downstream of port j+1 can be computed. Now we assume that it is acceptably accurate to assume no head loss across a port along the main, leading to

$$\frac{V_{j+1}^2}{2g} + \frac{p_{j+1}}{\gamma} = \frac{V_j^2}{2g} + \frac{p_j'}{\gamma} \tag{3.27}$$

This last assumption may be questionable for the first two or three ports at the downstream end, but thereafter it should be a very good and slightly conservative assumption. The right side of this equation is entirely known. Since p_{aj+1} can be determined, then E_{j+1} is known, but the two terms on the left side of Eq. 3.27 are not yet separately known. Consequently we can not immediately find C_D at port j+1, since Eq. 3.24 shows that we must know the upstream velocity head to do that. So we proceed as follows.

If we know q_{j+1}, then

$$Q_{j+1} = Q_j + q_{j+1} \tag{3.28}$$

and V_{j+1} can be found directly. But Eq. 3.22 clearly requires a value for C_{Dj+1}. We can iterate our way to a solution by first computing an estimate of q_{j+1} as

$$q_{j+1} = C_{Dj} a_{j+1}\left(2gE_{j+1}\right)^{1/2} \tag{3.29}$$

with C_{Dj} based on $\left(V_j^2/2g\right)/E_{j+1}$ instead of $\left(V_{j+1}^2/2g\right)/E_{j+1}$, and then in turn computing Q_{j+1} from Eq. 3.28, V_{j+1} from Q_{j+1}, and then an improved value of C_{Dj+1} based on V_{j+1}. This cycle will almost always converge in one or two iterations to give an accurate value of C_D at port j+1. This computational routine is used at each port.

This computational routine is repeated from one port to the next until the entire manifold has been traversed. At this point the total head has been computed at the upstream end of the manifold. For the manifold to function as the computations indicate, this head or a larger head must be supplied to this point. Commonly the goal is either to match some head here to a reservoir head or the head from a pumping plant, and the computed total will rarely be the same as the target head. Two approaches are available for the reconciliation of this difference: (1) Recognizing in the entire computational procedure

that heads are proportional to the square of the velocities or discharges, all discharges can be proportionally scaled, as was demonstrated in Example Problem 3.1,

$$Q_{true} = Q_{est}\left[\frac{H_{true}}{H_{est}}\right]^{1/2} \tag{3.30}$$

in which H_{true} is the desired target head, Q_{est} and H_{est} are the estimated discharges and heads that are the outcome of the computation, and Q_{true} are the discharges that will produce the desired head. (2) The other approach is simpler but still effective, and that is simply to raise or lower the original head at port 1 in proportion to the amount by which the target head is missed in the previous trial and to rerun the problem with the computer program; continue these adjustments until the target head is met with acceptable accuracy.

Computer programs that perform this sequence of computations have been developed by various individuals and organizations. Grace (1978, pp. 296-297) presents a typical set of plots that are the outcome of such studies; the plots display the relatively small variation of discharge from port to port that is attainable by good design. A relatively simple version of a typical manifold program has been written and will be found with the other programs on the CD in file MANIFOLD. A study of the program listing should help the reader understand the details of implementing the computational procedure. The current program follows the methodology in this section, including the neglect of head loss at a port along the main. But the code also indicates where modifications are needed to include this factor, if it is to be added to the program.

3.4 PROBLEMS

3.1 In the manifold shown below, neglect all losses except pipe friction in the barrel, and assume $f = 0.02$ is a reasonable estimate for the Darcy friction factor in the barrel.

(a) Assume the discharge from each port i is $Q_i = 0.35$ ft^3/s. Compute each port diameter d_i, $i = 1,4$, that is required so that the assumption of equal discharges is true.
(b) Now assume that all four port diameters are each the size d_1 that was computed in part (a) and compute the resulting discharge Q_i from each port.

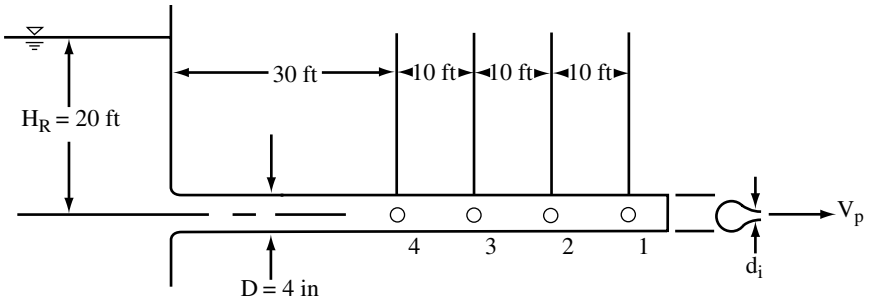

3.2 It is proposed to distribute water to irrigation furrows on two sides of a road, as shown in the next figure, by a system which is supplied by an elevated reservoir and consists of one 12-in-diameter used pipe (still in good condition) that serves both sides of the road via many circular holes or ports on 5-ft intervals. The largest port diameter is to be 2.0 in. Each port is to discharge 0.2 ft^3/s. Assuming for simplicity that $f = 0.02$ is a suitable friction factor and neglecting junction and other minor losses, estimate the required water surface elevation in the reservoir to fulfill these requirements.

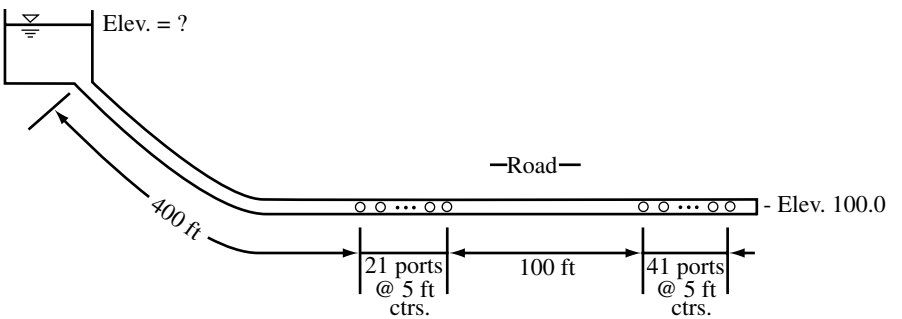

3.3 Consider n equally-spaced ports in a length L of pipe having diameter D and friction factor f. Assume equal discharge q from each port.

(a) Including friction but not junction losses, is it possible for the hydraulic grade line to have the same elevation at both ends of the manifold section of the pipe? Conclude "yes" or "no" and then justify your answer by using equations.
(b) Does conclusion (a) depend on the overall discharge Q in the manifold, or is your conclusion independent of discharge?
(c) If condition (a) were realized and q is constant, does this mean that each port diameter must be the same? Respond "yes" or "no" only.
(d) Comment briefly on whether a consideration of junction losses would alter your reply to part (a).

3.4 Compute the discharge from reservoir A to reservoir B for the system shown below. Assume $f = 0.02$ and neglect local losses. The pump characteristic curve can be represented by $h_p = 300 - 20Q^2$ with h_p in ft and Q in ft^3/s. Although the diameters of the intake ports are not stated, assume as an approximation that they cause the inflow over this section to be uniformly distributed.

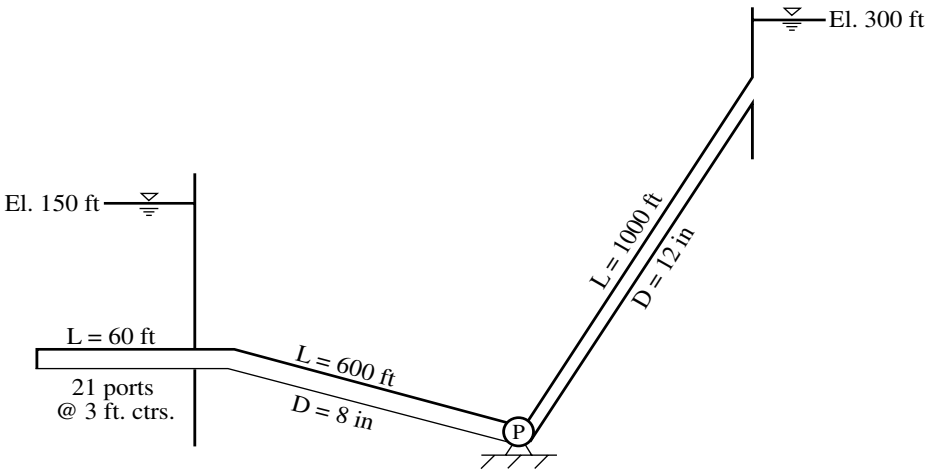

3.5 Consider again the manifold shown for Problem 3.1, but now do not neglect junction losses. The ratio of diameters between the laterals and the main is $D_3/D_1 = 0.2$, and the length of each lateral is 10 in. Assume $f = 0.025$.

(a) Using Fig. 3.5, develop and plot $K_{L1\text{-}2}$ vs. Q_3/Q_1. Does the coefficient become negative? Over what range of Q_3/Q_1?
(b) Develop a plot similar to Fig. 3.8 which displays C as a function of Q_3/Q_1.
(c) Starting with a trial EL of 10 ft, determine the discharge from each port and the total discharge from the manifold.
(d) What is the elevation of the actual EL downstream of the ports?

3.6 Certain assumptions are made in the analysis of a major submarine diffuser manifold for the disposal of wastewater. Indicate which of the following assumptions is both correct and justified, and why the others are in some way incorrect or not justified.

(a) All losses at a junction are ignored.
(b) At a junction only port losses are considered.
(c) Only losses along the main are considered at a junction.
(d) All losses at a junction usually should be considered.

3.7 A city treats at least some wastewater by overland flow. It is proposed to deliver 0.1 ft^3/s of dilute wastewater (same properties as water) through 50 ports, which are 5 feet apart, to the land surface. The main delivery line is old 8-inch-diameter metal pipe coming from a raised reservoir. You are asked to act as a consultant on the project.

(a) It is proposed that the diameter of each port opening be 1.25 inch because it is easy to build. Indicate whether this port size is an acceptable choice. Secondly, tell the project workers whether 0.1 ft^3/s can be delivered through each port this way.

(b) For a preliminary design assume $Q_p = 0.1$ ft^3/s from each port, $f = 0.02$ and neglect all local losses. Estimate the minimum reservoir surface elevation that can be used successfully here.
(c) Do you think a consideration of junction losses would significantly change your answer in part (b)? Do you think a more detailed analysis of the flow out each port is needed? In each case, why do you think so? Reply briefly to both questions, but do no additional calculations.

3.8 Devise a computational scheme to determine the head loss across a port in the main line of a manifold. Implement the scheme in the manifold program MANIFOLD on the CD, and test the scheme by running the program, using additional print statements to obtain enough information to verify that the program operates correctly.

3.9 Trickle irrigation of a field may involve a hierarchy of manifolds; that is, a delivery main can serve as the supply to several manifolds, and each manifold will in turn serve a number of laterals. Finally, each lateral will contain along its length a number of individual emitters. The manifold program on the CD is suitable for application to the pipes that are called manifolds in this application, so long as care is taken to treat the port exit pressures properly. However, each line called a lateral is itself a pipe containing numerous emitters or "ports" and so is itself a kind of manifold having two significant differences from the manifold which is modeled in the current manifold program: (1) At each port the trickle emitter usually (but not always) has a "barb" that projects into the main and causes a head loss at the port along the main; (2) Irrigation practitioners represent the discharge from an individual emitter by $q = KH^x$, in which K is a discharge coefficient that is characteristic of the emitter, H = pressure head = $(p - p_a)/\gamma$, and the exponent varies with the type of emitter over the range $0 \le x \le 0.8$. For example, for simple orifice or nozzle emitters $x = 0.5$. For more information see James (1988) or Keller and Bliesner (1990).

Modify the manifold program on the CD to simulate the flow in a trickle irrigation "lateral":
(a) For barb losses along the main, called the lateral, irrigation references (e.g. James 1988, p. 281) describe the head loss in terms of an equivalent additional pipe length. If the head loss along the main at a port is $h_L = KV^2/2g$, then the loss coefficient is of the form

$$K = Cf / D^m$$

with C being a pure number, f = Darcy friction factor, D = pipe inside diameter, and m = exponent, usually approximately 3.
(b) Replace the port discharge formula that is in the program with $q = KH^x$, and modify the program input statements to read the new data that are required.